mathematics

MDPI

Article

Optimal Power Dispatch of PV Generators in AC Distribution Networks by Considering Solar, Environmental, and Power Demand Conditions from Colombia

Luis Fernando Grisales-Noreña [1], Oscar Danilo Montoya [2,3,*], Brandon Cortés-Caicedo [4], Farhad Zishan [5] and Javier Rosero-García [6]

1 Department of Electrical Engineering, Faculty of Engineering, Universidad de Talca, Curicó 3340000, Chile
2 Grupo de Compatibilidad e Interferencia Electromagnética (GCEM), Facultad de Ingeniería, Universidad Distrital Francisco José de Caldas, Bogotá 110231, Colombia
3 Laboratorio Inteligente de Energía, Universidad Tecnológica de Bolívar, Cartagena 131001, Colombia
4 Departamento de Mecatrónica y Electromecánica, Facultad de Ingeniería, Instituto Tecnológico Metropolitano, Medellín 050036, Colombia
5 Department of Electrical Engineering, Sahand University of Technology, Tabriz 5513351996, Iran
6 Grupo de Investigación Electrical Machines & Drives (EM&D), Departamento de Ingeniería Eléctrica y Electrónica, Facultad de Ingeniería, Universidad Nacional de Colombia, Bogotá 111321, Colombia
* Correspondence: odmontoyag@udistrital.edu.co

Abstract: This paper deals with the problem regarding the optimal operation of photovoltaic (PV) generation sources in AC distribution networks with a single-phase structure, taking into consideration different objective functions. The problem is formulated as a multi-period optimal power flow applied to AC distribution grids, which generates a nonlinear programming (NLP) model with a non-convex structure. Three different objective functions are considered in the optimization model, each optimized using a single-objective function approach. These objective functions are (i) an operating costs function composed of the energy purchasing costs at the substation bus, added with the PV maintenance costs; (ii) the costs of energy losses; and (iii) the total CO_2 emissions at the substation bus. All these functions are minimized while considering a frame of operation of 24 h, i.e., in a day-ahead operation environment. To solve the NLP model representing the studied problem, the General Algebraic Modeling System (GAMS) and its SNOPT solver are used. Two different test feeders are used for all the numerical validations, one of them adapted to the urban operation characteristics in the Metropolitan Area of Medellín, which is composed of 33 nodes, and the other one adapted to isolated rural operating conditions, which has 27 nodes and is located in the department of Chocó, Colombia (municipality of Capurganá). Numerical comparisons with multiple combinatorial optimization methods (particle swarm optimization, the continuous genetic algorithm, the Vortex Search algorithm, and the Ant Lion Optimizer) demonstrate the effectiveness of the GAMS software to reach the optimal day-ahead dispatch of all the PV sources in both distribution grids.

Keywords: day-ahead operation of PV sources; energy purchasing costs; operation and maintenance costs of PV sources; energy losses costs; nonlinear programming formulation; GAMS software

MSC: 90C25; 90C26; 90C34

check for updates

Citation: Grisales-Noreña, L.F.; Montoya, O.D.; Cortés-Caicedo, B.; Zishan, F.; Rosero-García, J. Optimal Power Dispatch of PV Generators in AC Distribution Networks by Considering Solar, Environmental, and Power Demand Conditions from Colombia. *Mathematics* **2023**, *11*, 484. https://doi.org/10.3390/math11020484

Academic Editors: Kuo Tian, Weizhu Yang and Shiyao Lin

Received: 16 December 2022
Revised: 4 January 2023
Accepted: 9 January 2023
Published: 16 January 2023

1. Introduction

The massive integration of renewable energy in electrical networks is mandatory for all electricity industry participants nowadays since it is deemed imperative in reducing the harmful effects of global warming [1]. These renewable energy resources, which operate at all voltage levels, will reduce the energy purchasing costs and the multiple pollutants in the atmosphere, mainly produced by coal-, diesel-, or gas-based generation systems [2–4]. The most advanced, mature, and accepted technologies regarding renewable power sources are wind and solar generation, as many years of research have allowed for the development of robust generation systems that can be integrated into large-, medium-, and low-scale applications without affecting their efficiency [5–7], i.e., they can be connected at any voltage level (transmission, sub-transmission, and distribution levels) [8–11].

In the case of countries located between the tropics of Cancer and Capricorn, as is the case of Colombia, the most suitable generation technology based on renewables is photovoltaic (PV) generation [12]. This is due to the 11- to 13-h solar incidence in Colombia during the year, which is due to its proximity to the equatorial line [13]. This research focuses on a sub-problem related to PV generation sources in medium-voltage applications [14]. This problem corresponds to the day-ahead operation of these devices, taking into consideration aspects such as the geographical location of the PV sources (rural or urban distribution grids) and the different objective function indicators as a function of the grid operator requirements [15].

In the current literature, the problem regarding the optimal operation of renewable generation sources in distribution networks has been addressed by employing multiple approaches, some of which are discussed below. The authors of [16] presented an optimization model to locate and size PV generators and battery energy storage systems in medium-low voltage microgrids. The location of the PV sources and batteries was carried out using a simulated annealing algorithm. Once these devices are located, their daily operation was determined by using a conic formulation in order to minimize the energy purchasing and operating and maintenance costs of batteries. Numerical results demonstrated the efficiency of the proposed model in comparison to nonlinear programming (NLP) solvers in test feeders with 11, 135, and 230 nodes. In the work by [17], a mixed-integer conic model for locating and sizing PV sources in electrical AC distribution grids was presented while considering two main stages. The first stage defined the nodes where the PV sources were to be located and their expected sizes, considering the operation of the PV sources by tracking the maximum power point. In the second stage, the optimal sizes of the PV sources were refined, considering that the PV sources do not necessarily operate by tracking the maximum power point. The effectiveness of the proposed methodology was tested in the IEEE 33- and 69-bus grids and compared with multiple metaheuristics-based algorithms, which confirmed the effectiveness of the proposed conic formulation to locate and size PV sources in AC distribution grids. The authors of [18] presented a master-slave optimization methodology based on the vortex optimization algorithm and the successive approximations power flow method in order to locate and size PV generators in distribution networks with AC or DC configurations while employing maximum power point tracking. Numerical results in the IEEE 33- and IEEE 69-bus grids demonstrated the effectiveness of the proposed approach in comparison with the discrete-continuous version of the Chu & Beasley genetic algorithm (CBGA) proposed by [13]. The study by [19] proposed an efficient operation dispatch model for multiple distributed energy resources including PV solar panels, micro-turbines, wind turbines, fuel cells, battery energy storage systems, and controllable loads using a virtual power plant formulation. The main idea was to minimize the expected generation costs of the power system under analysis while considering uncertainties in the primary energy resources. The NLP model was solved with a new combinatorial optimizer named beetle antenna search, with better numerical performance when compared to particle swarm optimizers and genetic algorithms.

Considering the revision of the state of the art presented, this research article contributes with the following: (i) a general NLP formulation of the day-ahead operation problem for PV generation sources in AC single-phase distribution networks while considering different objective functions; (ii) a comparative analysis between different combinatorial optimization methods (i.e., as particle swarm optimization, the continuous genetic algorithm, the Vortex Search algorithm, and the Ant Lion Optimizer) and the exact solution of the NLP model using the GAMS software; and (iii) the best possible solution reported in the literature for the studied problem since the interior point with logarithmic barrier used in the NLP solution through GAMS ensures the optimum global finding.

It is worth mentioning that within the scope of this research,

i. the demand and PV generation curves in the regions of interest (the city of Medellín and the municipality of Capurganá) are considered as inputs for the NLP model, i.e., these predictions are assumed as constant values for the optimization model, which implies that no uncertainties regarding generation and demand curves are considered in this research;
ii. the internal optimization properties of the SNOPT solver in GAMS, which are based on interior-point methods, are not discussed in this research since the interior-point method is a well-known and strongly supported optimization method to deal with NLP problems; and
iii. generation and demands curves for rural and urban areas were obtained from public data [20–22], but the information of the test feeders (the IEEE 33- and 27-node systems) was taken from literature reports due to the restrictions imposed by distribution companies in Colombia on the use of real distribution grids.

The remainder of this research article is structured as follows: Section 2 presents the general mathematical formulation of the studied problem, i.e., the three different objective functions considered, as well as the set of constraints that make up its NLP formulation; Section 3 describes the general implementation of the NLP model in the GAMS software; Section 4 describes the main characteristics of the urban distribution grid (IEEE 33-bus grid) and the data obtained for the metropolitan area of Medelleín, as well as the rural distribution grid composed of 27 nodes and inspired by the rural area of Capurganá, Chocó, Colombia; Section 5 presents the main numerical results reached by the GAMS software and the SNOPT solver, as well as a complete comparison with different combinatorial optimization algorithms; and Section 6 presents the main concluding remarks derived from this work, as well as some possible future works.

2. General NLP Formulation

The problem regarding the optimal operation of PV generators in AC distribution networks can be represented as a day-ahead operation problem with different objective function indicators. The selection of each objective function depends on the optimization requirements of the distribution system operator. This study considers an NLP model with three possible objective functions to be minimized to represent the studied problem. The first objective function corresponds to the minimization of the total energy purchasing costs at the terminals of the substation, which is added to the operation and maintenance costs of the PV generation sources. The second objective function is defined as the minimization of the expected costs for the energy losses caused by all the resistive effects in all the branches of the distribution grid. Finally, the third objective function is related to minimizing the expected CO_2 emissions at the terminals of the substation bus. Note that all the aforementioned objective functions will be minimized based on a day-ahead operation approach, i.e., operation during a horizon of 24 h. Observe that Figure 1 illustrates the main aspects of the solution approach proposed in this research.

Figure 1 shows that (i) the NLP model regarding the optimal dispatch of PV sources in distribution networks requires knowing the nodes where the PV sources are located, the solar radiance and temperature (the area of influence of the distribution grid), and the expected behavior of the energy users (demand consumption profiles); and (ii) the NLP model was implemented in the GAMS software, which allows determining the best generation profiles for each distributed generator as a function of the objective function under analysis, i.e., economic, technical, or environmental performance indicators.

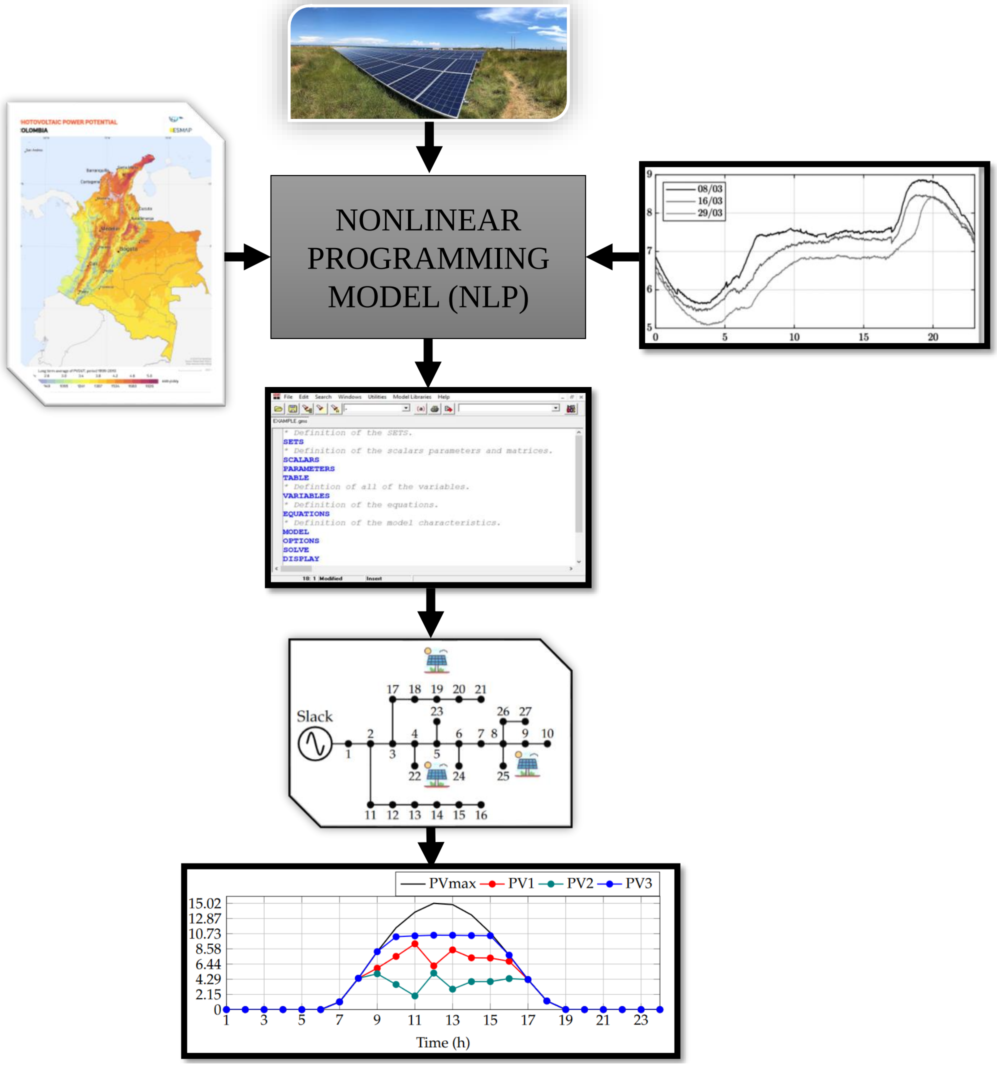

Figure 1. Main aspects of the proposed solution methodology.

Exact NLP model

The complete mathematical formulation of the studied problem is formulated in Equations (1)–(15).

Objective functions:

$$\min E_{cost} = C_{kWh}\left(\sum_{h\in\mathcal{H}}\sum_{i\in\mathcal{N}} p^{s}_{i,h}\Delta h\right) + C_{O\&M}\left(\sum_{h\in\mathcal{H}}\sum_{i\in\mathcal{N}} p^{pv}_{i,h}\Delta h\right) \tag{1}$$

$$\min E_{loss} = \sum_{h\in\mathcal{H}}\sum_{l\in\mathcal{L}} R_l I_l^2 \Delta h, \tag{2}$$

$$\min E_{CO_2} = CE_s\left(\sum_{h\in\mathcal{H}}\sum_{i\in\mathcal{N}} p^{s}_{i,h}\Delta h\right). \tag{3}$$

Set of constraints:

$$p^{s}_{i,h} + p^{pv}_{i,h} - P^{d}_{i,h} = \sum_{l \in \mathcal{L}} A_{i,l} \left(V^{re}_{i,h} I^{re}_{l,h} + V^{im}_{i,h} I^{im}_{l,h} \right), \quad \begin{Bmatrix} \forall i \in \mathcal{N}, \\ \forall h \in \mathcal{H} \end{Bmatrix}, \tag{4}$$

$$q^{s}_{i,h} - Q^{d}_{i,h} = - \sum_{l \in \mathcal{L}} A_{i,l} \left(V^{re}_{i,h} I^{im}_{l,h} - V^{im}_{i,h} I^{re}_{l,h} \right), \quad \begin{Bmatrix} \forall i \in \mathcal{N}, \\ \forall h \in \mathcal{H} \end{Bmatrix}, \tag{5}$$

$$P^{s,\min}_{i} \leq p^{s}_{i,h} \leq P^{s,\max}_{i}, \quad \begin{Bmatrix} \forall i \in \mathcal{N}, \\ \forall h \in \mathcal{H} \end{Bmatrix} \tag{6}$$

$$Q^{s,\min}_{i} \leq q^{s}_{i,h} \leq Q^{s,\max}_{i}, \quad \begin{Bmatrix} \forall i \in \mathcal{N}, \\ \forall h \in \mathcal{H} \end{Bmatrix}, \tag{7}$$

$$P^{pv,\min}_{i} \leq p^{pv}_{i,h} \leq P^{pv,\max}_{i}, \quad \begin{Bmatrix} \forall i \in \mathcal{N}, \\ \forall h \in \mathcal{H} \end{Bmatrix}, \tag{8}$$

$$I^{re}_{l,h} = \frac{1}{R_l^2 + X_l^2} \sum_{i \in \mathcal{N}} A_{i,l} \left(R_l V^{re}_{i,h} + X_l V^{im}_{i,h} \right), \quad \begin{Bmatrix} \forall l \in \mathcal{L}, \\ \forall h \in \mathcal{H} \end{Bmatrix}, \tag{9}$$

$$I^{im}_{l,h} = \frac{1}{R_l^2 + X_l^2} \sum_{i \in \mathcal{N}} A_{i,l} \left(R_l V^{im}_{i,h} - X_l V^{re}_{i,h} \right), \quad \begin{Bmatrix} \forall l \in \mathcal{L}, \\ \forall h \in \mathcal{H} \end{Bmatrix}, \tag{10}$$

$$V_{i,h} = \sqrt{\left(V^{re}_{i,h} \right)^2 + \left(V^{im}_{i,h} \right)^2}, \quad \begin{Bmatrix} \forall i \in \mathcal{N}, \\ \forall h \in \mathcal{H} \end{Bmatrix}, \tag{11}$$

$$I_{l,h} = \sqrt{\left(I^{re}_{l,h} \right)^2 + \left(I^{im}_{l,h} \right)^2}, \quad \begin{Bmatrix} \forall l \in \mathcal{L}, \\ \forall h \in \mathcal{H} \end{Bmatrix}, \tag{12}$$

$$V^{\min}_{i} \leq V_{i,h} \leq V^{\max}_{i}, \quad \begin{Bmatrix} \forall i \in \mathcal{N}, \\ \forall h \in \mathcal{H} \end{Bmatrix}, \tag{13}$$

$$0 \leq I_{l,h} \leq I^{\max}_{l}, \quad \begin{Bmatrix} \forall l \in \mathcal{L}, \\ \forall h \in \mathcal{H} \end{Bmatrix}, \tag{14}$$

$$p^{pv}_{i,h} \leq P^{pv}_{i} C^{pv}_{h}, \quad \begin{Bmatrix} \forall i \in \mathcal{N}, \\ \forall h \in \mathcal{H} \end{Bmatrix}. \tag{15}$$

The complete interpretation of the optimization model shown in (1)–(15) is as follows: Equation (1) corresponds to the first objective function regarding the minimization of the expected distribution grid operating costs, which includes the energy purchasing costs at the substation terminals, added with the operating costs of PV sources. Equation (2), the second objective function, is more related to a technical performance indicator used in optimizing distribution networks. It corresponds to the minimization of the expected daily energy losses associated with all the losses in the resistive parameters of the distribution lines for a daily operation environment. Equation (3) refers to the environmental performance indicator, an objective function that aims to minimize the greenhouse gas emissions (i.e., CO_2) to the atmosphere caused by conventional or diesel generation sources. Equality constraints (4) and (5) are known as the *power balance constraints*. These are entrusted with ensuring the power equilibrium at each node and for each period, i.e., they are the combination of Kirchhoff's first and second laws with Tellegen's second theorem [23]. Box-type inequality constraints (5) and (6) refer to the admissible lower and upper active and reactive power generation bounds of the conventional generation source connected to node i in the period h, respectively. Inequality constraint (8) defines the admissible generation region allowed for any PV source integrated to the distribution grid. Equality constraints (9) and (10) allow calculating the real and imaginary parts of the currents through the distribution line l as a function of the voltage variables and impedance parameters of the line, respectively. Equations (11) and (12) define the magnitudes of the voltage and current variables, respectively, as a function of their rectangular components.

Inequality constraints (13) and (14) are related to the voltage regulation limits imposed by regulatory policies and the maximum thermal limits associated with all the distribution lines, respectively. Finally, inequality constraint (15) shows that the PV generation units cannot necessarily work with maximum power point tracking as it will depend on the grid energy requirements.

Remark 1. *The following are the most important characteristics of the optimization model defined from (1) to (15):*

- *It is a nonlinear, non-convex optimization model due to the presence of products between the voltage and current variables in the power balance constraints, as well as square roots regarding voltage and current magnitudes.*
- *It is possible to find the optimal solution for each one of the single-objective function models by using the interior point method with logarithmic barriers, given that it is a continuous nonlinear programming model with quadratic constraints [24].*
- *The main effect in considering the grid nature (AC technology) in the optimization model is the presence of multiple nonlinear constraints regarding power equilibrium at each node and the presence of root square equalities regarding voltage variables, which become the optimization model highly complex in comparison to DC grids where the complexity of the optimization problem is reduced about 50% since no reactive power constraints and variables appear [25].*

This research focuses on (i) the solution of the exact NLP model in the GAMS through the SNOPT solver and (ii) the comparison of this solution with multiple combinatorial optimization algorithms such as the Vortex Search algorithm, CBGA, the particle swarm optimization method, and the Ant Lion Optimizer. In addition, two radial distribution networks with different operating conditions are considered, one with urban characteristics and the other in a rural area. The next section presents the main characteristics of the implementation of the exact NLP model (1)–(15) in the GAMS software.

3. Solution Methodology

This section presents two main aspects regarding the proposed solution methodology. The first corresponds to the general implementation of the exact NLP model in the GAMS software. The second corresponds to the general approach for calculating the PV generation inputs in a distribution network depending on the distribution grid's area of operation.

Remark 2. *The proposed optimization model (1)–(15) is solved in the research with the help of the GAMS software by considering a single-objective minimization procedure, i.e., each one of the objective functions in Equations (1) to (3) are minimized separately, and the other two ones are evaluated to know their final values. Note that more research regarding multi-objective optimization is required, and it can be an opportunity for research in future works.*

3.1. General Implementation of an NLP Model in the GAMS Software

To deal with the NLP model, shown in (1)–(15), this research selected the GAMS software to solve this optimization problem since, as demonstrated in multiple research articles, it can find the global optimum with its SNOPT solver if the optimization problem does not include discrete variables [26]. Multiple authors have successfully used the GAMS software to deal with complex NLP problems in engineering and science. The authors of [27] presented the solution to the problem regarding the optimal design of an osmotic generation plant in the Bahmanshir River of Iran, demonstrating excellent numerical results and low computational effort. The work by [28] addressed multiple optimization problems in power systems, which include the optimal dispatch with thermal plants and the optimal operation of batteries and energy storage systems in a market environment. Authors such as [29,30] have used the GAMS software to deal with the problem regarding the optimal placement and sizing of dispersed generation units in distribution networks, aiming to minimize the total grid power losses, with excellent numerical results when compared to those obtained via combinatorial optimization methods. The work by [31] presented a multi-objective optimization approach for the stack of a thermoacoustic engine using the GAMS as an optimization tool. In [32], an optimization model for a pump and valve schedule in complex water distribution networks was presented using GAMS Modeling Language. Finally, the authors of [33] used the GAMS software and the SNOPT solver to present the solution of an NLP problem regarding parametric estimation in single-phase transformers while considering voltage and current measures.

The literature above confirms that the GAMS optimization package efficiently deals with complex optimization problems, especially if they are defined in the continuous domain. This tool can find the optimal global solution by combining interior point methods with logarithmic barriers and gradient-based optimizers. Figure 2 presents the general structure in implementing an NLP model in the GAMS software.

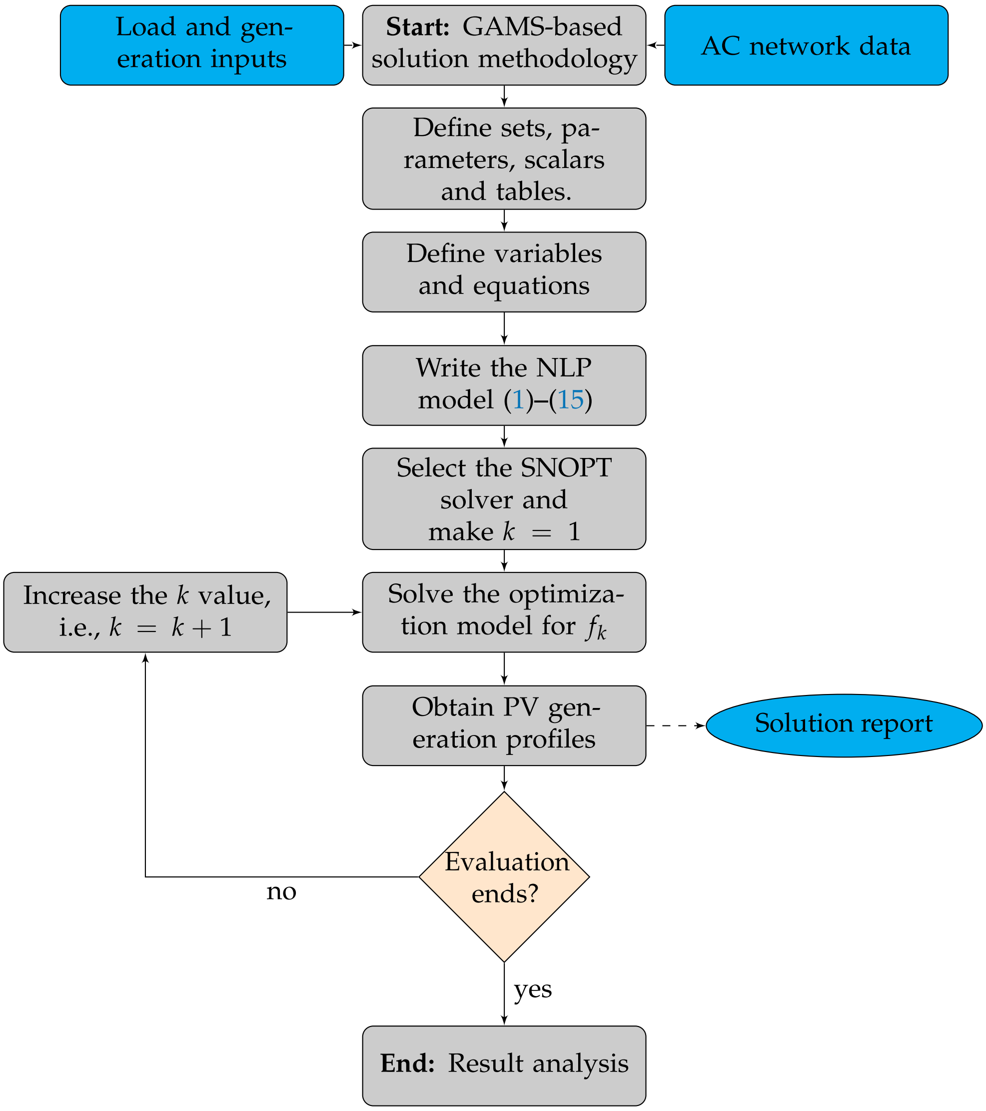

Figure 2. General steps for implementing an NLP model in the GAMS software.

Remark 3. *Note that the value of f_k is defined as the objective function of interest, i.e., $f_1 = E_{cost}$, $f_2 = E_{loss}$, and $f_3 = E_{CO_2}$. This implies that the flow diagram in Figure 2 is a general solution methodology that allows solving the NLP model (1)–(15) for different objective functions.*

3.2. Adjusting the Solar Generation Curves

The main characteristic of PV-technology-based solar generation is its dependence on weather conditions, i.e., the solar radiation and temperature exposition of the panels [34].

In addition, due to the sudden variations in solar incidence for a particular area, e.g., due to cloud movements, generation based on PV systems is considered a non-dispatchable source [35]. This implies that for the daily economic dispatch analysis, it is mandatory to correctly predict the PV generation availability [26]. There are multiple literature reports that nonlinearly relate solar radiation and temperature to predict the total power output of a PV system [36]. This study adopts the formulation reported by [37] in obtaining the expected power production of a PV system.

$$p_{i,h}^{pv} = P_i^{pv} f_{pv} \left(\frac{G_h^T}{G_i^{T,STC}} \right) \left[1 + \alpha_p \left(T_{i,h}^c - T_i^{c,STC} \right) \right], \tag{16}$$

Note that in (16), it is observed that the total power output of a PV generation system is indeed a nonlinear function of the current system temperature, solar radiation, and some factors associated with the expected efficiency of the complete generation system.

To determine the surface temperature of the panels that compose the PV system, Equation (17) is used.

$$T_{i,h}^c = T_h^a + G_h^T \left(\frac{T_i^{c,NOCT} - T_i^{a,NOCT}}{G_i^{T,NOCT}} \right) \left(1 - \frac{\eta_i^c}{\alpha} \right) \tag{17}$$

To find the expected behavior of solar generation in the urban and rural areas under analysis, this research considers the parametric information presented in Table 1. Note that this information was adapted from [37,38], assuming that the panel was constructed with silicon polycrystalline technology.

Table 1. Parametric information regarding PV generation sources.

Parameter	Value	Unit	Parameter	Value	Unit
P_i^{pv}	1	W	f_{pv}	0.95	-
$G_i^{T,STC}$	1000	W/m^2	α_p	-0.0045	1/°C
$T_i^{c,STC}$	25	°C	$T_i^{c,NOCT}$	46	°C
$G_i^{T,NOCT}$	800	W/m^2	$T_i^{a,NOCT}$	20	°C
η_i^c	0.141	-	$\tau\alpha$	0.9	-

It is worth mentioning that if one considers the total power output of the PV system under nominal operating conditions as $1W$, then the expected generation will be defined in the interval $[0, 1]$, i.e., and it can be considered as percentage generation curve. Note that this curve represents the C_h^{pv} parameter and is an input in the proposed NLP model (1)–(15).

4. Generation and Demand Parametrization of the Urban and Rural Zones

To evaluate the effectiveness of the proposed GAMS-based optimization approach at operating dispersed generation based on PV generation for AC distribution networks, this study considers two types of operation areas: i.e., an urban area and a rural area. The first area of operation corresponds to the metropolitan area of Medellín, the second largest city of Colombia in terms of population. The second region corresponds to a rural area located on the Pacific coast of Colombia, i.e., the Municipality of Capurganá in the department of Chocó.

4.1. Urban and Rural Generation Curves

To characterize the power generation of the metropolitan area of Medellín, solar radiation and ambient temperature data provided by the National Aeronautics and Space Administration's (NASA) database were considered [20]. Note that this information was defined in 2019, i.e., 1 January to 31 December, taking a 1-h resolution into account. This average information is presented in Table 2. In addition, if Equations (16) and (17) are considered for the information reported in Table 1, then the average power output generation for Medellín is as presented in Table 2 and Figure 3.

Remark 4. *The information available in the NASA database is also considered to obtain the generation curve for the municipality of Capurganá, and the same procedure is followed. The complete generation profile for this area is also reported in Table 2 and Figure 3.*

Table 2. Solar radiation data (W/m^2), ambient temperature (°C), and behavior (p.u.) for an average day in the regions under study.

Region	**Medellín**			**Capurganá**		
Hour	G_T	T_a	C_{pv}	G_T	T_a	C_{pv}
1	0	16.14132	0	0	24.44252	0
2	0	15.90636	0	0	24.32474	0
3	0	15.68132	0	0	24.22545	0
4	0	15.46022	0	0	24.14674	0
5	0	15.27545	0	0	24.08422	0
6	0	15.10329	0	0	24.03482	0
7	46.02425	15.15718	0.04541	29.14570	24.10367	0.02770
8	190.83559	16.15636	0.18424	142.11066	24.78126	0.13277
9	362.83753	17.43868	0.34100	291.61926	25.68211	0.26622
10	526.64647	18.87312	0.48161	431.95384	26.63671	0.38547
11	640.99058	20.27438	0.57375	540.61581	27.47515	0.47362
12	709.05312	21.36342	0.62572	605.16362	28.10252	0.52397
13	701.86370	21.98721	0.61809	606.93027	28.46775	0.52442
14	626.82690	22.12107	0.55716	583.07479	28.56923	0.50519
15	499.86074	21.83071	0.45236	490.55904	28.42334	0.43065
16	346.26581	21.20351	0.32052	359.22033	28.03460	0.32148
17	186.66671	20.38668	0.17693	204.48775	27.44945	0.18722
18	52.33403	19.35951	0.05066	64.51775	26.69008	0.06034
19	0.50986	18.32258	0.00050	3.17460	25.89016	0.00300
20	0	17.72414	0	0	25.39227	0
21	0	17.29586	0	0	25.09285	0
22	0	16.96148	0	0	24.87663	0
23	0	16.67395	0	0	24.70841	0
24	0	16.40545	0	0	24.56926	0

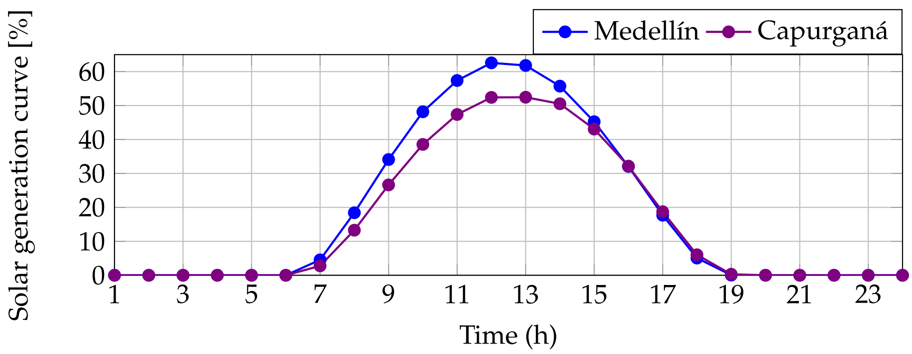

Figure 3. Expected generation profiles for Medellín and Capurganá, Colombia.

4.2. Urban and Rural Demand Curves

To determine the expected energy consumption profiles in the areas of interest, this study considers the consumption information provided by the distribution companies that operate in these areas:

i. Medellín: The historical reports made by the network operator Empresas Públicas de Medellín (EPM) [22] were considered. Consumption data for 2019 were taken, i.e., from 1 January to 31 December, with a 1-h sampling. As for the power generation curves, the data collected were averaged per hour, as shown in Table 3. With the data consigned in this table, the average behavior of power consumption for a typical day in Medellín was obtained, as shown in Figure 4 and Table 3.

ii. Capurganá: Power consumption data were taken from the reports of historical events by the IPSE [21], which is in charge of monitoring and supervising the non-interconnected electrical areas of Colombia in order to promote, develop, and implement energy-related solutions in these areas. As in the previous case, the collected data were averaged per hour as shown in Table 3. Similarly, it is possible to obtain the average consumption behavior for a typical day in Capurganá, as shown in Figure 4 and Table 3.

Table 3. Power consumption data (kW) and behavior (p.u.) for an average day in the regions under study.

Region	Medellín		Capurganá	
Hour	P_d	$P_{d,pu}$	P_d	$P_{d,pu}$
1	1,012,876.20	0.65509	428.04117	0.84573
2	974,315.40	0.63015	409.76717	0.80962
3	951,768.01	0.61557	317.81654	0.62795
4	952,169.92	0.61583	256.70648	0.50720
5	996,601.97	0.64457	51.70864	0.10217
6	1,080,667.80	0.69894	11.05835	0.02185
7	1,135,234.91	0.73423	32.49553	0.06421
8	1,226,850.93	0.79348	62.77491	0.12403
9	1,303,895.33	0.84331	119.17381	0.23547
10	1,354,781.01	0.87622	281.26057	0.55572
11	1,417,860.03	0.91702	333.09429	0.65813
12	1,462,589.11	0.94595	358.36076	0.70805
13	1,459,381.62	0.94388	368.01140	0.72712
14	1,439,889.28	0.93127	369.70917	0.73048
15	1,430,823.70	0.92541	379.97901	0.75077
16	1,426,481.64	0.92260	388.65478	0.76791
17	1,404,019.24	0.90807	386.78365	0.76421
18	1,373,896.43	0.88859	395.19266	0.78083
19	1,463,002.74	0.94622	430.88177	0.85134
20	1,478,398.44	0.95618	464.61670	0.91800
21	1,415,579.31	0.91555	476.40313	0.94128
22	1,310,824.08	0.84779	473.67462	0.93589
23	1,187,930.28	0.76831	467.29281	0.92328
24	1,086,900.38	0.70297	452.18590	0.89344

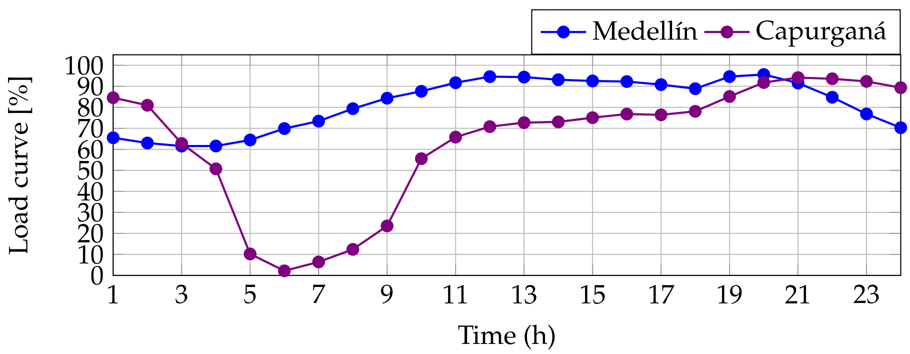

Figure 4. Expected energy consumption profiles for Medellín and Capurganá, Colombia.

4.3. Parametrization of the Optimization Model

To calculate the objective function values defined in Equations (1)–(3), the information reported in Table 4 is employed. Note that this table presents the costs of generating energy in urban and rural areas. In the same way, the costs associated with the maintenance of PV generation systems are shown.

Table 4. Parameters to evaluate the objective function in the proposed NLP formulation.

Parameter	Value	Unit	Parameter	Value	Unit
C_{kWh}^{Urban}	0.1302	USD/kWh	CE_s^{Urban}	0.1644	kg/kWh
C_{kWh}^{Rural}	0.2913	USD/kWh	CE_s^{Rural}	0.2671	kg/kWh
$C_{O\&M}^{pv}$	0.0019	USD/kWh	-	-	-

It is worth noting the following:

i. The energy generation costs in the urban and rural areas were taken from the reports made by the network operators to the Unified Information System (SUI by its Spanish acronym) in 2019 [39,40].
ii. The operation and maintenance costs of the PV generators were taken from [41].
iii. The emissions factor for the urban area is the one established by XM for the interconnected electrical system, to which Empresas Públicas de Medellín (EPM) belongs [42]. Similarly, the emissions factor for the rural area is the one associated with diesel fuel and was taken from the database of the Emission Factors of Colombian Fuels (FECOC, by its Spanish acronym) [43].

Remark 5. *The voltage regulation bounds for electrical systems with a voltage level greater than* $1kV$ *and less than* $62kV$*, i.e., medium-voltage networks, are defined as* $+5$ *and* -10% *of the nominal voltage. These bounds are established by the 1340 Colombian Technical Standard (NTC, by its Spanish acronym) [44].*

5. Test Systems

To evaluate the proposed NLP formulation to operate PV generation systems in urban and rural environments while considering different objective functions, two test feeders were considered. The first one is the IEEE 33-bus grid, which was employed to emulate the distribution operating conditions of the city of Medellín. The second one is a 27-bus grid originally designed for rural simulation environments, which is adapted in this research to analyze the municipality of Capurganá. To define the nodes where the PV generators are located, we consider that these were previously selected in distribution system planning studies carried out by the distribution company. In this research, the information regarding PV sources' location and sizes has been obtained from [18].

5.1. Urban Simulation Test System

For this simulation case, the IEEE 33-bus test feeder is considered. This distribution system is composed of 33 nodes and 32 distribution lines, and it is operated at the substation terminals with a nominal voltage of 12.66 kV. The electrical topology of the IEEE 33-bus grid is presented in Figure 5 [45]. Note that to evaluate the effect of the PV generation in this system, three PV sources with nominal rates of 2400 kW were added to nodes 12, 15, and 31, respectively.

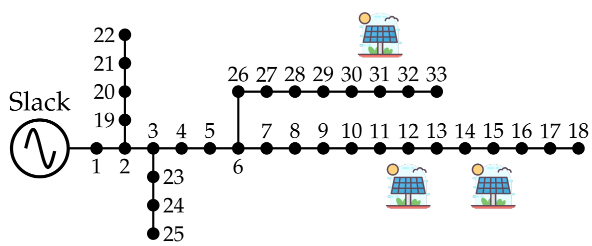

Figure 5. Proposed configuration of the IEEE 33-bus grid for simulating the operation scenario in the city of Medellín.

In addition, the parametric information regarding peak loads and branch parameters are listed in Table 5. It is worth mentioning that to evaluate the current constraints in the optimization model (1)–(15), the power flow solution under peak load conditions is used, which provides the maximum currents through each distribution line. With these currents, the conductors that can be assigned to these lines, according to the Colombian regulation NTC 2050, are found, assuming that they will operate under a nominal temperature of 60 °C.

Table 5. Information regarding the peak load conditions, impedance parameters, and current bounds of the IEEE 33-bus grid.

Line l	Node i	Node j	R_{ij} (Ω)	X_{ij} (Ω)	P_j (kW)	Q_j (kvar)	$I_l^{\max}$ (A)
1	1	2	0.0922	0.0477	100	60	385
2	2	3	0.4930	0.2511	90	40	355
3	3	4	0.3660	0.1864	120	80	240
4	4	5	0.3811	0.1941	60	30	240
5	5	6	0.8190	0.7070	60	20	240
6	6	7	0.1872	0.6188	200	100	110
7	7	8	1.7114	1.2351	200	100	85
8	8	9	1.0300	0.7400	60	20	70
9	9	10	1.0400	0.7400	60	20	70
10	10	11	0.1966	0.0650	45	30	55
11	11	12	0.3744	0.1238	60	35	55
12	12	13	1.4680	1.1550	60	35	55
13	13	14	0.5416	0.7129	120	80	40
14	14	15	0.5910	0.5260	60	10	25
15	15	16	0.7463	0.5450	60	20	20
16	16	17	1.2890	1.7210	60	20	20
17	17	18	0.7320	0.5740	90	40	20
18	2	19	0.1640	0.1565	90	40	40
19	19	20	1.5042	1.3554	90	40	25
20	20	21	0.4095	0.4784	90	40	20
21	21	22	0.7089	0.9373	90	40	20
22	3	23	0.4512	0.3083	90	50	85
23	23	24	0.8980	0.7091	420	200	85
24	24	25	0.8960	0.7011	420	200	40
25	6	26	0.2030	0.1034	60	25	125
26	26	27	0.2842	0.1447	60	25	110
27	27	28	1.0590	0.9337	60	20	110
28	28	29	0.8042	0.7006	120	70	110
29	29	30	0.5075	0.2585	200	600	95
30	30	31	0.9744	0.9630	150	70	55
31	31	32	0.3105	0.3619	210	100	30
32	32	33	0.3410	0.5302	60	40	20

5.2. Rural Simulation Test System

The 27-bus grid is a radial distribution network composed of 27 nodes and 26 distribution lines, which operate with a nominal voltage of 23 kV at the substation terminals. This test feeder was proposed initially by the authors of [46] to evaluate the problem regarding the optimal selection of conductors. The electrical configuration of this test feeder is reported in Figure 6. Note that this system has three PV generators, all with a nominal power of 2400 kW, located at nodes 5, 9, and 19.

Due to the fact that the 27-bus grid was initially proposed to determine the optimal conductor sizes, the thermal bounds for each distribution line are also taken from [46]. The complete parametric information of this test feeder is reported in Table 6.

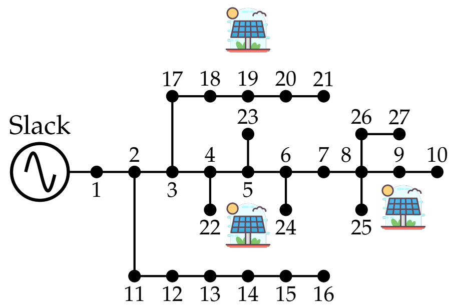

Figure 6. Proposed configuration of the 27-bus grid to simulate the operation scenario in the municipality of Capurganá.

Table 6. Information regarding peak load conditions, impedance parameters, and current bounds for the 27-bus grid.

Line l	Node i	Node j	R_{ij} (Ω)	X_{ij} (Ω)	P_j (kW)	Q_j (kvar)	$I_l^{\max}$ (A)
1	1	2	0.0140	0.6051	0	0	240
2	2	3	0.7463	1.0783	0	0	165
3	3	4	0.4052	0.5855	297.50	184.37	95
4	4	5	1.1524	1.6650	0	0	85
5	5	6	0.5261	0.7601	255.00	158.03	70
6	6	7	0.7127	1.0296	0	0	55
7	7	8	1.6628	2.4024	212.50	131.70	55
8	8	9	5.3434	3.1320	0	0	20
9	9	10	2.1522	1.2615	266.05	164.88	20
10	2	11	0.4052	0.5855	85.00	52.68	70
11	11	12	1.1524	1.6650	340	210.71	70
12	12	13	0.5261	0.7601	297.50	184.37	55
13	13	14	1.2358	1.1332	191.25	118.53	30
14	14	15	2.8835	2.6440	106.25	65.85	20
15	15	16	5.3434	3.1320	255.00	158.03	20
16	3	17	1.2942	1.1867	255.00	158.03	70
17	17	18	0.7027	0.6443	127.50	79.02	55
18	18	19	3.3234	1.9480	297.50	184.37	40
19	19	20	1.5172	0.8893	340	210.71	25
20	20	21	0.7127	1.0296	85.00	52.68	20
21	4	22	8.2528	2.9911	106.25	65.85	20
22	5	23	9.1961	3.3330	55.25	34.24	20
23	6	24	0.7463	1.0783	69.70	43.20	20
24	8	25	2.0112	0.7289	255.00	158.03	20
25	8	26	3.3234	1.9480	63.75	39.51	20
26	26	27	0.5261	0.7601	170	105.36	20

6. Numerical Results and Discussions

The general NLP model that represents the problem regarding the optimal operation of PV generation in AC distribution networks has been implemented and solved in the GAMS optimization package with the SNOPT solver on a Dell Precision 3450 workstation with an Intel(R) Core(TM) i9-11900 CPU@2.50 Ghz processor, 64.0 GB RAM and a Windows 10 Pro 64-bit operating system. To demonstrate the efficiency of the GAMS software in operating PV generators in AC distribution networks, its results were compared with those of different combinatorial optimization techniques such as particle swarm optimization (PSO) [47], the CBGA [48], the Vortex Search algorithm (VSA) [49], and the Ant Lion Optimizer (ALO) [50]. These methodologies were selected due to their excellent performance in solving the optimal power flow problem in electrical distribution systems [18,51–53]. In addition, to ensure a fair comparison between the SNOPT solver and the combinatorial algorithms, each of them was tuned in order to guarantee the best performance when solving the studied problem. Regarding the selection of parameters, the CBGA was used with an initial population of 40 individuals and a maximum number of iterations of 400.

6.1. Urban Test System Simulations

Table 7 shows the numerical results of all the combinatorial optimization algorithms and the SNOPT solver applied to the IEEE 33-bus grid. The information in this table is presented from left to right, as follows: the methodology used, the value obtained for the evaluated function, and the average computation time.

Table 7. Numerical results in the 33-bus system for the urban zone.

Method	f_1(USD)	f_2(kWh)	f_3(kg CO_2)	Proc. Time f_1(s)	Proc. Time f_2(s)	Proc. Time f_3(s)
Bench. Case	9931.66	3379.07	12,541.22	-	-	-
CBGA	7409.25	2346.00	9309.57	2.6258	2.6054	2.6236
PSO	7317.89	2332.05	9198.27	31.4035	31.9980	30.0664
VSA	7276.05	2331.61	9152.05	42.4710	37.9801	43.9550
ALO	7220.09	2331.51	9068.94	141.9966	140.1495	140.5316
SNOPT	7219.93	2331.48	9068.75	0.3450	0.3180	0.2830

The numerical results for the urban test system show that the SNOPT solver finds the best solution with respect to all the other methods. The following facts can be observed: (i) The final total operating costs of the network are 7219.93 USD, that is, an improvement of 2711.73 USD regarding the base case, 189.31 USD regarding the CBGA, 97.96 USD regarding PSO, 56.11 USD regarding the VSA, and 0.15 USD regarding the ALO; (ii) the final energy losses of the network are 2331.48 kWh, showing an improvement of 1047.59 kWh with respect to the base case, 14.52 kWh with respect to the CBGA, 0.57 kWh with respect to PSO, 0.13 kWh with respect to the VSA, and 0.03 kWh with respect to the ALO; and (iii) as for CO_2 emissions, the SNOPT solver achieves a response of 9068.75 kg of CO_2, evidencing an improvement of 3472.47 kg of CO_2 with respect to the base case, 240.82 kg of CO_2 with respect to the CBGA, 129.51 kg of CO_2 compared to PSO, 83.30 kg of CO_2 compared to VSA, and 0.18 kg of CO_2 with respect to the ALO.

Similarly, it is evident that the SNOPT solver is the fastest methodology in the three simulation scenarios for the urban test system. The SNOPT solver takes approximately 0.3450 s to calculate f_1, 0.3180 s to calculate f_2, and 0.2830 s to calculate f_3. This shows that in order to solve a multidimensional (i.e., 39-dimensional) NLP model with continuous variables (solution space with infinite combinations), the SNOPT solver takes less than 0.50 s to converge to the optimal solution.

Regarding the daily expected improvements in the proposed objective functions, Figure 7 presents the percentage of reductions reached by each method with respect to the base case.

Figure 7 shows that all optimization techniques allow for a reduction of more than 25% compared to the base case for the three simulation scenarios. The SNOPT solver allows the highest objective function reduction for the three simulation scenarios, i.e., 27.30, 31, and 27.68%. On the other hand, all the combinatorial optimization methods exhibit very good performance. However, due to their random nature, these algorithms are trapped in locally optimal solutions, and statistical analysis is required to ensure that they reach good solutions on average.

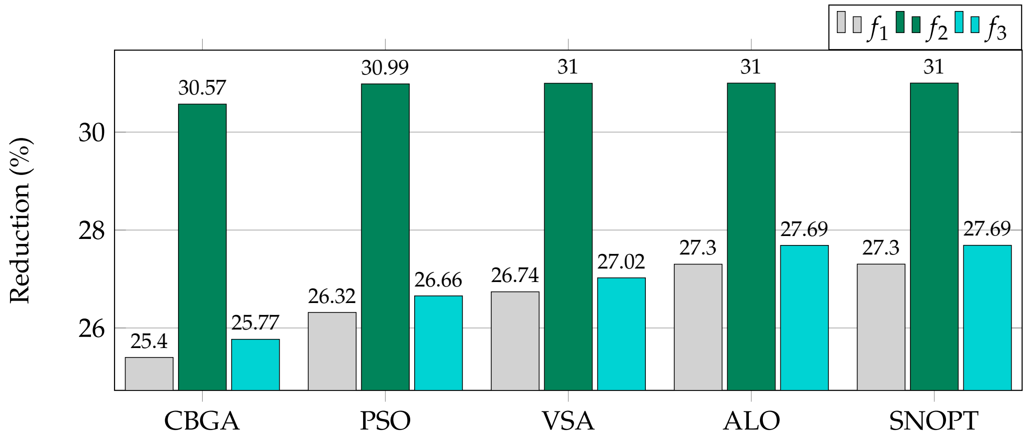

Figure 7. Reduction percentage regarding the objective functions in the IEEE 33-bus system.

Remark 6. *The above demonstrates the effectiveness and robustness of the SNOPT solver when solving the problem regarding the operation of PV generators in AC distribution networks, which allows optimizing the system from an economic, technical, or environmental point of view. The exact solution obtains the best performance when it comes to the best response and processing times (less than 0.50 s). This turns the proposed approach into the best option to address this problem with regard to the urban test system, obtaining a global optimal solution for each simulation scenario, which respects the technical operating conditions of the network.*

6.2. Rural Test System Simulations

Table 8 shows the numerical performance of all the combinatorial optimization algorithms and the SNOPT solver for the 27-bus grid in rural applications. Note that this table has the same information shown in Table 7.

Table 8. Numerical results in the 27-bus system for the rural zone.

Method	f_1(USD)	f_2(kWh)	f_3(kg CO_2)	Proc. Time f_1(s)	Proc. Time f_2(s)	Proc. Time f_3(s)
Bench. Case	18,543.84	691.15	17,005.21	-	-	-
CBGA	12,282.02	559.51	11,192.67	1.8066	1.8311	1.8213
PSO	12,104.61	558.28	11,064.72	21.8934	27.804	21.0702
VSA	12,052.94	558.22	11,023.51	30.7303	30.2881	30.4519
ALO	12,022.40	558.20	10,985.75	125.9021	126.5206	131.3081
SNOPT	12,022.34	558.20	10,985.71	0.2990	0.2850	0.2410

The numerical results for the IEEE 27-bus grid show that the SNOPT solver finds the best solution with respect to all methods used: (i) for f_1, the SNOPT solver exhibits a response of 12,022.34 USD, i.e., an improvement of 6521.50 USD regarding the base case, 259.68 USD regarding the CBGA, 82.27 USD regarding PSO, 30.60 USD regarding the VSA, and 0.06 USD regarding the ALO; (ii) in the case of the f_2 function, the SNOPT solver reaches a response of 558.20 kWh, showing an improvement of 132.95 kWh with respect to the base case, 1.31 kWh with respect to the CBGA, 0.08 kWh with respect to PSO, 0.02 kWh with respect to the VSA, and 0.00 kWh with respect to the ALO; and (iii) in the case of f_3, the SNOPT shows a response of 10,985.71 kg of CO_2, evidencing an improvement of 6019.50 kg of CO_2 with respect to the base case, 206.96 kg of CO_2 with respect to the CBGA, 79.01 kg of CO_2 with respect to PSO, 37.80 kg of CO_2 with respect to VSA, and 0.04 kg of CO_2 with respect to the ALO.

It is worth mentioning that the SNOPT solver is the fastest methodology to solve the problem of optimal PV operation in the rural test system with regard to the proposed objective functions. The SNOPT solver takes approximately 0.2990 s to calculate f_1, 0.2850 s to calculate f_2, and 0.2410 s to calculate f_3, thus showing that the GAMS approach takes less than 0.3 s to reach the optimal global solution of a complex problem from a dimensional and solution space perspective. In addition, Figure 8 depicts the expected reduction percentage reached by each method when compared to the base case.

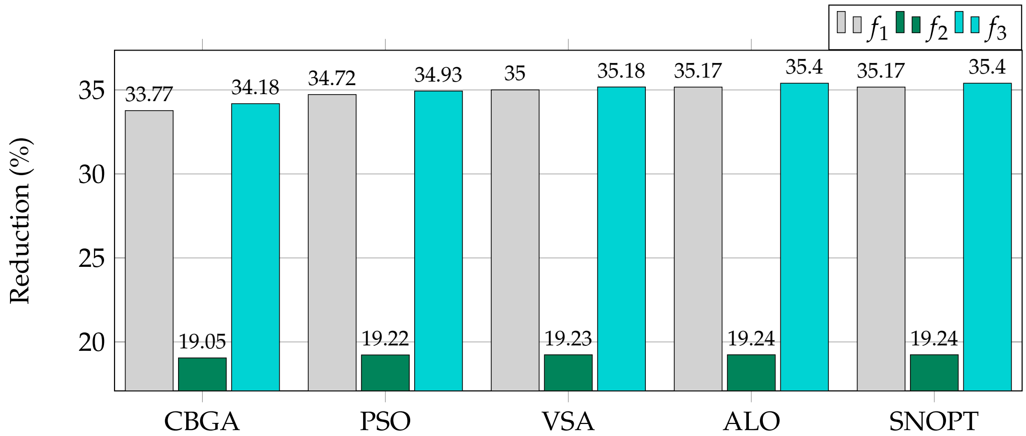

Figure 8. Reduction percentage regarding the objective functions in the IEEE 27-bus system.

In the rural case, all optimization techniques allow for a reduction of more than 18.5% compared to the base case for the three simulation scenarios. The SNOPT solver achieves the highest objective function reduction for the three simulation scenarios, i.e., 35.17, 19.27, and 35.40%. All the combinatorial optimization methods are adequate in solving the problem under study. However, they yield locally optimal solutions due to the randomness of the exploration and exploitation of the solution space.

Remark 7. *The results obtained for the rural test system indicate that the SNOPT solver has the best performance, namely, better response and processing times (less than 0.3 s). This makes this solution methodology the best option to address the problem of operating PV generators in the IEEE 27-bus grid as it obtains an optimal global solution for each simulation scenario, which respects the technical-operating conditions of the network.*

7. Conclusions and Future Work

The problem regarding the optimal daily operation dispatch of PV generation units in electrical distribution networks was addressed in this research by implementing its NLP model in the GAMS software with the SNOPT solver. Numerical results in two test feeders composed of 27 and 33 nodes demonstrated the effectiveness and robustness of the GAMS software in dealing with the global optimal solution while considering three different objective functions, i.e., the daily operating costs of energy purchasing at the substation bus, added with the maintenance and operation costs of the PV sources; the total daily energy losses caused by the resistive effects in all the distribution lines; and the total CO_2 emissions (kg) at the substation bus.

A complete characterization of two different operation areas in Colombia was proposed in order to evaluate the proposed solution approach in urban and rural areas. The IEEE 33-bus grid was adapted to the operating conditions of the metropolitan area of Medellín, Antioquia, Colombia, and the 27-bus grid was set with the operating conditions of the municipality of Capurganá, Chocó. Information regarding solar radiation and temperature in 2019 was obtained from the NASA database in order to determine the potential for solar power generation in both areas. In addition, an accurate PV model was adjusted to consider the external effects on the effective power generation output. To characterize the demand behavior, the information provided by the utility company of Medellín (i.e., EPM) and the IPSE for the non-interconnected area were used to define the daily expected consumption profile of the urban and rural areas of analysis, respectively.

Numerical results showed the following: (i) For the urban simulation scenario, the SNOPT solver finds reductions of about 27.3039, 31.0022, and 27.6884% with respect to the f_1, f_2, and f_3 benchmark cases, respectively. In the case of the rural system, these reductions were 35.1680, 19.2358, and 35.3980%, respectively. In comparison with the combinatorial optimization methods used for validating the proposed approach, only the ALO approach reached a similar numerical performance while the other optimizers were stuck in locally optimal solutions due to the complexity of the NLP model and the infinite size of the solution space. (ii) Regarding the processing times, the SNOPT solver takes about 0.50 s to solve each one of the objective functions in both distribution grids, while the second best approach (i.e., the ALO approach) takes more than 120 s to reach its solutions. This confirms that the proposed approach finds the global optimal solution 240 times faster than the ALO approach with no need for statistical analysis, which was required by all the metaheuristic-based approaches in order to find the average performance and quality.

In future works, it will be possible to develop the following derived works: (i) extending the proposed NLP model to include battery energy storage systems and dynamic reactive power compensators; (ii) proposing a convex reformulation of the NLP model via conic or semidefinite programming in order to ensure that the global optimum is found; (iii) extending the proposed formulations to DC distribution networks with monopolar and bipolar structures; and (iv) the development of a comparative analysis of the proposed NLP model with other alternatives for modeling the PV sources and the power balance equations in distribution networks including uncertainties in demand and generation curves.

Author Contributions: Conceptualization, methodology, software, and writing (review and editing), L.F.G.-N., O.D.M., B.C.-C., F.Z. and J.R.-G. All authors have read and agreed to the published version of the manuscript.

Funding: This research was supported by Electrical Machines & Drives research Group (EM&D) from Universidad Nacional and project Think Green on the island of San Andres, BPIN 2016000100002 EEDAS ESP.

Data Availability Statement: Not applicable.

Conflicts of Interest: The authors of this paper declare no conflict of interest.

Abbreviations

The following abbreviations are used in this manuscript:

E_{cost}	Objective function associated with the total operating costs of the distribution grid (USD/day).
f_1	Component of the objective function related to the purchase of energy at the terminals of the substation node (USD/day).
f_2	Component of the objective function associated with the operation and maintenance costs of the PV generators (USD/day).
C_{kWh}	Average cost of purchasing power at the substation node (USD/Wh).
$p^s_{i,h}$	Active power generated by a conventional source connected to a node i during a period h (W).
Δh	Time in which the electrical variables are assumed to be constant (h).
$C_{O\&M}$	Maintenance and operation costs of a PV generator (USD/Wh).
$p^{pv}_{i,h}$	Active power generated by a PV source connected to a node i during a period h (W).
$\mathcal{N}$	Set that contains all the nodes of the network.
$\mathcal{H}$	Set that contains all periods in a daily operation scenario.
E_{loss}	Energy losses costs for a day of operation (USD/day).
R_l	Resistance associated with the distribution line l (Ω).
X_l	Reactance associated with the distribution line l (Ω).
I_l	Magnitude of the current that flows through the distribution line l (A).
$\mathcal{L}$	Set that contains all the distribution lines of the distribution network.

E_{CO_2}	Total greenhouse gas emissions per day of operation ($kgCO_2/day$).
CE_s	Factor of CO_2 emissions associated with conventional generation sources ($kgCO_2/W$).
$P^d_{i,h}$	Active power demanded at a node i for a period of time h (W).
$Q^d_{i,h}$	Reactive power demanded at a node i for a period of time h (var).
$q^s_{i,h}$	Reactive power generated by a conventional source connected to a node i during a period of time h (var).
$V^{re}_{i,h}$	Real part of the voltage profile at a node i during a period of time h (V).
$V^{im}_{i,h}$	Imaginary part of the voltage profile at a node i during a period of time h (V).
$I^{re}_{i,h}$	Real part of the current flowing through the line l during a period of time h (A).
$I^{im}_{i,h}$	Imaginary part of the current flowing through the line l during a period of time h (A).
$A_{i,l}$	Node-to-branch incidence matrix.
$P^{s,\min}_i$	Minimum active power bound associated with each conventional generator connected to node i (W).
$P^{s,\max}_i$	Maximum active power bound associated with each conventional generator connected to node i (W).
$Q^{s,\min}_i$	Minimum reactive power bound associated with each conventional generator connected to node i (var).
$Q^{s,\max}_i$	Maximum reactive power bound associated with each conventional generator connected to node i (var).
$P^{pv,\min}_i$	Minimum active power bound associated with each PV generator connected to node i (W).
$P^{pv,\max}_i$	Maximum active power bound associated with each PV generator connected to node i (W).
$V^{\min}_i$	Minimum voltage regulation bound associated with the voltage profile at node i (V).
$V^{\max}_i$	Maximum voltage regulation bound associated with the voltage profile at node i (V).
P^{pv}_i	Nominal power of the PV generator located at a node i (W).
C^{pv}_h	Expected PV generation behavior for the area where the distribution grid is located (p.u.).
f_{pv}	Reduction factor of the PV system's power output. It models the external effects that affect generation in PV systems (%).
G^T_h	Solar radiation that falls on a PV generator during a period of time h (W/m^2).
$G^{T,STC}_i$	Solar radiation of the PV generator located at node i under standard test conditions (W/m^2).
α_p	Coefficient regarding the power and temperature output ($1/°C$).
$T^c_{i,h}$	Real surface temperature of the PV generator located at node i during a period of time h (°C).
$T^{c,STC}_i$	Expected surface temperature of the PV generators located at node i under standard test conditions (°C).
T^a_h	Ambient temperature to which the PV generator is exposed during a period h (°C).
$T^{c,NOCT}_i$	Nominal surface temperature of the PV generator located at node i (when it is exposed to a radiation $G^{T,NOCT}_i$ and a temperature $T^{a,NOCT}_i$) (°C).
η^c_i	Electrical efficiency of the PV generator located at a node i (%).
τ	Solar transmittance parameter of the PV generator.
α	Solar absorption coefficient of the PV generator.

References

1. Ahmed, I.; Rehan, M.; Basit, A.; Hong, K.S. Greenhouse gases emission reduction for electric power generation sector by efficient dispatching of thermal plants integrated with renewable systems. *Sci. Rep.* **2022**, *12*, 12380. [CrossRef] [PubMed]
2. Jakhrani, A.Q.; Othman, A.K.; Rigit, A.R.H.; Samo, S.R. Estimation of carbon footprints from diesel generator emissions. In Proceedings of the 2012 International Conference on Green and Ubiquitous Technology, Besancon, France, 20–23 November 2012. [CrossRef]
3. Issa, M.; Ibrahim, H.; Hosni, H.; Ilinca, A.; Rezkallah, M. Effects of Low Charge and Environmental Conditions on Diesel Generators Operation. *Eng* **2020**, *1*, 137–152. [CrossRef]
4. Yang, L.; Sun, Q.; Zhang, N.; Li, Y. Indirect Multi-Energy Transactions of Energy Internet With Deep Reinforcement Learning Approach. *IEEE Trans. Power Syst.* **2022**, *37*, 4067–4077. [CrossRef]
5. Ahmad, L.; Khordehgah, N.; Malinauskaite, J.; Jouhara, H. Recent advances and applications of solar photovoltaics and thermal technologies. *Energy* **2020**, *207*, 118254. [CrossRef]

6. Tan, J.D.; Chang, C.C.W.; Bhuiyan, M.A.S.; Minhad, K.N.; Ali, K. Advancements of wind energy conversion systems for low-wind urban environments: A review. *Energy Rep.* **2022**, *8*, 3406–3414. [CrossRef]
7. Zhang, N.; Sun, Q.; Yang, L.; Li, Y. Event-Triggered Distributed Hybrid Control Scheme for the Integrated Energy System. *IEEE Trans. Ind. Inform.* **2022**, *18*, 835–846. [CrossRef]
8. Aybar-Mejía, M.; Villanueva, J.; Mariano-Hernández, D.; Santos, F.; Molina-García, A. A Review of Low-Voltage Renewable Microgrids: Generation Forecasting and Demand-Side Management Strategies. *Electronics* **2021**, *10*, 2093. [CrossRef]
9. Shafiullah, G. Impacts of renewable energy integration into the high voltage (HV) networks. In Proceedings of the 2016 4th International Conference on the Development in the in Renewable Energy Technology (ICDRET), Shenzhen, China, 30–31 December 2016. [CrossRef]
10. Zheng, H.; Yuan, X.; Cai, J.; Sun, P.; Zhou, L. Large-Signal Stability Analysis of DC Side of VSC-HVDC System Based on Estimation of Domain of Attraction. *IEEE Trans. Power Syst.* **2022**, *37*, 3630–3641. [CrossRef]
11. Surinkaew, T.; Ngamroo, I. Coordinated Robust Control of DFIG Wind Turbine and PSS for Stabilization of Power Oscillations Considering System Uncertainties. *IEEE Trans. Sustain. Energy* **2014**, *5*, 823–833. [CrossRef]
12. López, A.R.; Krumm, A.; Schattenhofer, L.; Burandt, T.; Montoya, F.C.; Oberländer, N.; Oei, P.Y. Solar PV generation in Colombia - A qualitative and quantitative approach to analyze the potential of solar energy market. *Renew. Energy* **2020**, *148*, 1266–1279. [CrossRef]
13. Montoya, O.D.; Grisales-Noreña, L.F.; Perea-Moreno, A.J. Optimal Investments in PV Sources for Grid-Connected Distribution Networks: An Application of the Discrete–Continuous Genetic Algorithm. *Sustainability* **2021**, *13*, 13633. [CrossRef]
14. Saidi, A.S. Impact of grid-tied photovoltaic systems on voltage stability of tunisian distribution networks using dynamic reactive power control. *Ain Shams Eng. J.* **2022**, *13*, 101537. [CrossRef]
15. Schultz, H.S.; Carvalho, M. Design, Greenhouse Emissions, and Environmental Payback of a Photovoltaic Solar Energy System. *Energies* **2022**, *15*, 6098. [CrossRef]
16. Valencia, A.; Hincapie, R.A.; Gallego, R.A. Optimal location, selection, and operation of battery energy storage systems and renewable distributed generation in medium–low voltage distribution networks. *J. Energy Storage* **2021**, *34*, 102158. [CrossRef]
17. Montoya, O.D.; Ramos-Paja, C.A.; Grisales-Noreña, L.F. An Efficient Methodology for Locating and Sizing PV Generators in Radial Distribution Networks Using a Mixed-Integer Conic Relaxation. *Mathematics* **2022**, *10*, 2626. [CrossRef]
18. Cortés-Caicedo, B.; Molina-Martin, F.; Grisales-Noreña, L.F.; Montoya, O.D.; Hernández, J.C. Optimal Design of PV Systems in Electrical Distribution Networks by Minimizing the Annual Equivalent Operative Costs through the Discrete-Continuous Vortex Search Algorithm. *Sensors* **2022**, *22*, 851. [CrossRef]
19. Pal, P.; Krishnamoorthy, P.A.; Rukmani, D.K.; Antony, S.J.; Ocheme, S.; Subramanian, U.; Elavarasan, R.M.; Das, N.; Hasanien, H.M. Optimal Dispatch Strategy of Virtual Power Plant for Day-Ahead Market Framework. *Appl. Sci.* **2021**, *11*, 3814. [CrossRef]
20. NASA. NASA Prediction of Worldwide Energy Resources. Available online: https://power.larc.nasa.gov/ (accessed on 21 September 2022).
21. Instituto de Planificación y Promoción de Soluciones Energéticas para Zonas No Interconectadas. Informes Mensuales de Telimetría, Colombia. Available online: https://ipse.gov.co/cnm/informe-mensuales-telemetria/ (accessed on 21 September 2022).
22. XM SA ESP. Sinergox Database, Colombia. Available online: https://sinergox.xm.com.co/Paginas/Home.aspx (accessed on 21 September 2022).
23. Zagirnyak, M.; Rodkin, D.; Romashykhin, I. The possibilities of Tellegen's theorem in the identification electrotechnical problems. In Proceedings of the 2017 International Conference on Modern Electrical and Energy Systems (MEES), Kremenchuk, Ukraine, 15–17 November 2017. [CrossRef]
24. El-Sobky, B.; Abo-Elnaga, Y.; Mousa, A.A.A.; El-Shorbagy, M.A. Trust-Region Based Penalty Barrier Algorithm for Constrained Nonlinear Programming Problems: An Application of Design of Minimum Cost Canal Sections. *Mathematics* **2021**, *9*, 1551. [CrossRef]
25. Grisales-Noreña, L.F.; Rosales-Mu noz, A.A.; Cortés-Caicedo, B.; Montoya, O.D.; Andrade, F. Optimal Operation of PV Sources in DC Grids for Improving Technical, Economical, and Environmental Conditions by Using Vortex Search Algorithm and a Matrix Hourly Power Flow. *Mathematics* **2022**, *11*, 93. [CrossRef]
26. Montoya, O.D.; Gil-González, W. Dynamic active and reactive power compensation in distribution networks with batteries: A day-ahead economic dispatch approach. *Comput. Electr. Eng.* **2020**, *85*, 106710. [CrossRef]
27. Naghiloo, A.; Abbaspour, M.; Mohammadi-Ivatloo, B.; Bakhtari, K. GAMS based approach for optimal design and sizing of a pressure retarded osmosis power plant in Bahmanshir river of Iran. *Renew. Sustain. Energy Rev.* **2015**, *52*, 1559–1565. [CrossRef]
28. Soroudi, A. *Power System Optimization Modeling in GAMS*; Springer International Publishing: Berlin/Heidelberg, Germany, 2017. [CrossRef]
29. Montoya, O.D.; Gil-González, W.; Grisales-Noreña, L. An exact MINLP model for optimal location and sizing of DGs in distribution networks: A general algebraic modeling system approach. *Ain Shams Eng. J.* **2020**, *11*, 409–418. [CrossRef]
30. Kaur, S.; Kumbhar, G.; Sharma, J. A MINLP technique for optimal placement of multiple DG units in distribution systems. *Int. J. Electr. Power Energy Syst.* **2014**, *63*, 609–617. [CrossRef]
31. Tartibu, L.; Sun, B.; Kaunda, M. Multi-objective optimization of the stack of a thermoacoustic engine using GAMS. *Appl. Soft Comput.* **2015**, *28*, 30–43. [CrossRef]

32. Skworcow, P.; Paluszczyszyn, D.; Ulanicki, B.; Rudek, R.; Belrain, T. Optimisation of Pump and Valve Schedules in Complex Large-scale Water Distribution Systems Using GAMS Modelling Language. *Procedia Eng.* **2014**, *70*, 1566–1574. [CrossRef]
33. Bocanegra, S.Y.; Montoya, O.D.; Molina-Cabrera, A. Parameter estimation in singe-phase transformers employing voltage and current measures (In Spanish). *Rev. Uis Ing.* **2020**, *19*, 63–75. [CrossRef]
34. Dubey, S.; Sarvaiya, J.N.; Seshadri, B. Temperature Dependent Photovoltaic (PV) Efficiency and Its Effect on PV Production in the World—A Review. *Energy Procedia* **2013**, *33*, 311–321. [CrossRef]
35. Jaya, S.; Vijay, A.S.; Khan, I.; Shukla, A.; Doolla, S. Mode Transition in DC Microgrids with Non-Dispatchable Sources. In Proceedings of the 2021 IEEE Energy Conversion Congress and Exposition (ECCE). IEEE, Vancouver, BC, Canada, 10–14 October 2021. [CrossRef]
36. Ramirez-Vergara, J.; Bosman, L.B.; Leon-Salas, W.D.; Wollega, E. Ambient temperature and solar irradiance forecasting prediction horizon sensitivity analysis. *Mach. Learn. Appl.* **2021**, *6*, 100128. [CrossRef]
37. Hassan, Q.; Jaszczur, M.; Przenzak, E.; Abdulateef, J. The PV cell temperature effect on the energy production and module efficiency. *Contemp. Probl. Power Eng. Environ. Prot.* **2016**, *33*, 33–40.
38. Schwingshackl, C.; Petitta, M.; Wagner, J.; Belluardo, G.; Moser, D.; Castelli, M.; Zebisch, M.; Tetzlaff, A. Wind Effect on PV Module Temperature: Analysis of Different Techniques for an Accurate Estimation. *Energy Procedia* **2013**, *40*, 77–86. [CrossRef]
39. Sistema Único de Información de Servicios Públicos Domicialiarios. Consolidado de Energía por Empresa y Departamento, Colombia. Available online: https://sui.superservicios.gov.co/Reportes-del-sector/Energia/Reportes-comerciales/Consolidado-de-energia-por-empresa-y-departamento (accessed on 21 September 2022).
40. Sistema Único de Información de Servicios Públicos Domicialiarios. Consolidado de Información Técnica Operativa ZNI, Colombia. Available online: https://sui.superservicios.gov.co/Reportes-del-sector/Energia/Reportes-comerciales/Consolidado-de-informacion-tecnica-operativa-ZNI (accessed on 21 September 2022).
41. Wang, P.; Wang, W.; Xu, D. Optimal Sizing of Distributed Generations in DC Microgrids With Comprehensive Consideration of System Operation Modes and Operation Targets. *IEEE Access* **2018**, *6*, 31129–31140. [CrossRef]
42. XM SA EPS. En Colombia Factor de Emisión de CO_2 por Generación eléCtrica del Sistema Interconectado: 164.38 Gramos de CO_2 por Kilovatio Hora, Colombia. Available online: https://www.xm.com.co/noticias/en-colombia-factor-de-emision-de-co2-por-generacion-electrica-del-sistema-interconectado (accessed on 21 September 2022).
43. Academia Colombiana de Ciencias Exactas, Físicas y Naturales. Factores de Emisión de los Combustibles Colombianos, Colombia, 2016. Available online: https://www.scribd.com/document/157258400/18-FECOC-factores-emision-colombia-docx# (accessed on 21 September 2022).
44. Normas Técnicas y Certificación (ICONTEC). *Tensiones y Frecuencia Nominales en Sistemas de Energía Elécrica en Redes de Servicio Público NTC1340*; ICONTEC: Bogotá, Colombia, 2004.
45. Baran, M.; Wu, F. Network reconfiguration in distribution systems for loss reduction and load balancing. *IEEE Trans. Power Deliv.* **1989**, *4*, 1401–1407. [CrossRef]
46. Falaghi, H.; Ramezani, M.; Haghifam, M.R.; Milani, K. Optimal selection of conductors in radial distribution systems with time varying load. In Proceedings of the 18th International Conference and Exhibition on Electricity Distribution (CIRED 2005), Turin, Italy, 6–9 June 2005. [CrossRef]
47. Eberhart, R.; Kennedy, J. Particle swarm optimization. In Proceedings of the IEEE International Conference on Neural Networks, Perth, WA, Australia, 27 November–1 December 1995; Citeseer: Piscataway, NJ, USA, 1995; Volume 4, pp. 1942–1948.
48. Chu, P.C.; Beasley, J.E. A genetic algorithm for the multidimensional knapsack problem. *J. Heuristics* **1998**, *4*, 63–86. [CrossRef]
49. Doğan, B.; Ölmez, T. A new metaheuristic for numerical function optimization: Vortex Search algorithm. *Inf. Sci.* **2015**, *293*, 125–145. [CrossRef]
50. Mirjalili, S. The ant lion optimizer. *Adv. Eng. Softw.* **2015**, *83*, 80–98. [CrossRef]
51. Wicaksana, M.G.S.; Putranto, L.M.; Waskito, F.; Yasirroni, M. Optimal placement and sizing of PV as DG for losses minimization using PSO algorithm: A case in Purworejo area. In Proceedings of the 2020 International Conference on Sustainable Energy Engineering and Application (ICSEEA), Online, 18–20 November 2020; pp. 1–6.
52. KS, G.D. Hybrid genetic algorithm and particle swarm optimization algorithm for optimal power flow in power system. *J. Comput. Mech. Power Syst. Control* **2019**, *2*, 31–37.
53. Ramavath, D.; Sharma, M. Optimal Power Flow Using Modified ALO. In Proceedings of the 2020 International Conference on Renewable Energy Integration into Smart Grids: A Multidisciplinary Approach to Technology Modelling and Simulation (ICREISG), Bhubaneshwar, India, 14–15 February 2020; pp. 84–89.